Tet Controls Axon Guidance in Early Brain Development through Glutamatergic Signaling

Hiep Tran[1], Le Le[1], Badri Nath Singh[1], Joseph Kramer[3], Ruth Steward[1, 2, *]

[1] Waksman Institute, Rutgers University, Piscataway, NJ 08854

[2]Department of Molecular Biology and Biochemistry, Cancer Institute of New Jersey, Rutgers University, New Brunswick, NJ 08901

[3]Department of Pathology and Laboratory Medicine, Rutgers Biomedical and Health Sciences, Rutgers University, New Brunswick, NJ 08901

* Corresponding author: Ruth Steward

Email: steward@waksman.rutgers.edu

Keywords: Tet, axon guidance, brain development, glutamatergic signaling, insulin-producing cells

Abstract

Ten-eleven translocation (Tet) is an important gene in neurodevelopment, but how Tet regulates brain development is still under study. Mutations in human TET proteins have been found in individuals with neurodevelopmental disorders. Here we report a new function of Tet in regulating *Drosophila* early brain development. We found that mutation on the Tet DNA-binding domain (Tet^{AXXC}) resulted in axon guidance defects in the mushroom body (MB). Tet is required in early brain development during the outgrowth of MB β axons. Transcriptomic study of Tet^{AXXC} mutant and wild-type pupal brains shows that glutamine synthetase 2 (Gs2), a key enzyme in glutamatergic signaling, is the most significantly down-regulated gene in the *Tet* mutant brains. RNAi knockdown or CRISPR/Cas9 mutagenesis of Gs2 recapitulates the Tet^{AXXC} phenotype. Surprisingly, Tet and Gs2 act in the insulin-producing cells (IPCs) to control MB axon guidance, and overexpression of Gs2 in the IPCs rescue the axonal defects of Tet^{AXXC}. Treating Tet^{AXXC} with the metabotropic glutamate receptor antagonist MPEP can also rescue the phenotype confirming Tet function in regulating glutamatergic signaling. Tet^{AXXC} and the *Drosophila* homolog of *Fragile X Messenger Ribonucleoprotein protein* mutant ($Fmr1^3$) have similar mushroom body axonal defects and reduction in Gs2 transcription, and, importantly, overexpression of Gs2 in the IPCs of Fmr1 mutants also rescues the axonal defects. Our studies reveal a new function of Tet in regulating axon guidance in the brain via glutamatergic signaling and suggest overlapping functions between Tet and Fmr1.

Introduction

Ten-eleven translocation (TET) is one of the most important epigenetic and epitranscriptomic regulators. TET can convert 5mC to 5hmC (1), which is the first step in DNA demethylation. Through this enzymatic activity, Tet promotes transcription by maintaining genes in a hypomethylated stage (2). In recent years, TET was shown to also convert 5mrC to 5hmrC in mRNA. This modification positively influences the translational efficiency of mRNAs (3-5). Most vertebrates such as humans and mice have three TET genes while other metazoans, including fruit fly *Drosophila melanogaster,* have only one Tet gene (6). However, *Drosophila* Tet encodes two Tet isoforms, Tet-L and Tet-S, through separate promoters (7). Tet-L has both a CXXC zinc finger DNA-binding-domain and a dioxygenase catalytic domain, which are highly conserved (6). Tet-S lacks the DNA-binding domain but otherwise contains the same protein sequence as Tet-L (7). Loss of all three TET genes in mice leads to embryonic lethality (8). In *Drosophila,* Tet^{null} mutants can live through embryogenesis and all three larval stages but fail to eclose from the pupal case after the adult body is formed (7). Recently, TET mutations in humans have been linked to neurodevelopmental disorders (ND) associated with intellectual disability (ID) and autism spectrum disorders (ASD) (9-12). The mechanisms underlying these neurodevelopmental disorders have not been elucidated.

Drosophila Tet is highly expressed in the developing nervous system and Tet RNAi knockdown in the brain produces defects in larval locomotion and adult circadian rhythm (7). However, it was unclear how Tet regulates the development of the early brain. One key process during brain development is axon guidance, as the correct wiring of axons will determine the neural circuits in the adult brain (13), and mis-regulation axon guidance can lead to neurodevelopmental disorders (14). To test whether Tet functions in axon guidance, we used a well-studied axonal structure in the *Drosophila* brain, the mushroom body (MB).

The insect MB is the analogous structure of the human hippocampus (15). In *Drosophila*, the MB is responsible for several important brain functions including learning and memory, circadian rhythms, sleep, and courtship behavior (16, 17). Each MB structure derives from four embryonic MB neuroblasts (MBNBs) (18). During embryogenesis, larval, and pupal development, these MBNBs sequentially generate different classes of MB neurons or Kenyon Cells (KCs) whose axons later form γ, α′/β′, and α/β lobes in adult brain (18). These MB lobes can be divided into 15 compartments and each compartment is connected to specific MB output neurons or dopaminergic neurons as part of the brain circuit in order to modulate a variety of brain functions (16). Thus, the axonal projection in each lobe is highly regulated to ensure proper brain circuitry.

Glutamate is the major excitatory neurotransmitter and has a key role in various neurological processes such as development, neuronal plasticity, and learning and memory (19-21). The NMDA-type glutamate receptors (NMDARs) are present in axons and growth cones of young hippocampal neurons (22) and misregulation of the metabotropic glutamate receptors (mGluRs) signaling causes neuronal defect (23). Glutamate levels can affect the growth rate and branching of dopaminergic neurons *in vitro* (24). Interestingly, the responsiveness of growth cones to repellent molecules such as slit-

2, semaphoring 3A, and semaphoring 3C is dependent on the levels of glutamate in the culture medium (25). GABA is the main inhibitory neurotransmitter in the brain that also plays an important role in development and neuronal activity (26, 27). However, the mechanism in which glutamatergic and GABAergic regulate axon guidance in the brain are not well understood.

Fragile X Messenger Ribonucleoprotein 1 (FMR1) is a human gene encoding the Fragile X Messenger Ribonucleoprotein (FMRP) which is important for regulating synaptic plasticity, protein synthesis, and dendritic morphology (28). In patients with Fragile X syndrome (FXS), the most common form of inherited intellectual and developmental disability, the gene generally is silenced by CGG trinucleotide expansion leading to promoter hypermethylation (28). FMR1 is conserved in *Drosophila* and mutants in the *Fmr1* homolog have been used to study the requirement of the gene and to identify potential therapeutic treatments for FXS (29, 30). The *Drosophila Fmr1* mutants have been shown to have defects in axon guidance and to affect neurological functions such as learning and memory as well as courtship behavior (23, 31).

In this study, we investigate a new function of Tet in regulating brain development. Tet can control MB axon guidance at the midline of the central brain by regulating glutamine synthetase 2 (Gs2), a key enzyme in glutamatergic signaling. The regulation occurs when MB axons are forming in the early pupal brain. Our results show that the *Tet* and *Fmr1* mutant phenotype can be rescued by expressing Gs2 in the insulin-producing cells (IPCs) located at the midline of the brain.

Results

Loss of Tet results in mushroom body axon fusion

The *Drosophila* adult mushroom body (MB) is a prominent structure in the insect brain. In the normal brain, the β lobes are separated at the brain midline, e.g., the β lobe in the left-brain hemisphere never touches the β lobe on the right side (**Fig. 1A**). To test whether Tet is required in the MB axons, we knocked down its expression using an RNAi line under the control of 201Y-GAL4. This Gal4 driver is expressed in γ neurons and α/β core neurons of the MB and was previously recombined with a UAS-CD8::GFP construct to visualize both the cell body and axons of MB neurons (32). Knockdown of Tet did not affect the γ lobes (**SI Appendix Fig. S1A, B**) or α lobes (**Fig. 1C-G**), but strikingly, the Tet knockdown using 201Y-GAL4 causes MB β lobes to cross the midline and fuse with the β lobe from the opposite brain hemisphere (compare **Fig. 1C, E, G** with **Fig. 1B, D, F)**. 71% (n=31) of Tet RNAi flies show β lobe fusion while none of the RNAi control flies showed fusion (n=29) (**Fig. 1H**). Thus, Tet is required in 201Y-expressing cells to inhibit β lobe axons from crossing the midline.

The Tet CXXC zinc finger domain is required for normal β axon development

Tet proteins have two key domains, the CXXC zinc finger domain, and the 2OGFeDO catalytic domain. Mammalian TET CXXC zinc finger domains can bind to DNA to modulate epigenetic marks or to recruit other epigenetic factors to regulate gene expression (2, 33, 34). The 2OGFeDO domain is responsible for converting 5-methylcytosine (5mC) to 5-hydroxymethylcytosine (5hmC) in both DNA and RNA (1, 3). To investigate if these domains have distinct functions, we employed a CRISPR/Cas9 and homologous directed repair (HDR) approach to generate targeted point mutations (35-37). A previous study had shown that mutating one cysteine in the highly conserved zinc finger domain of the CGBP (CpG-binding protein) protein to alanine completely abolished its ability to bind DNA (**Fig.1I**) (38). We generated a mutant fly line in which the same conserved cysteine within Tet was substituted by alanine (Tet^{AXXC})(**Fig.1I**). Using the same CRISPR/Cas9 and HDR approach, we also generated a mutant in which the conserved histidine and aspartic acid in the active site of the catalytic domain were substituted by tyrosine and alanine (Tet^{YRA}) (**Fig. 1J**). This change in amino acids was previously shown to abolish the catalytic function of vertebrate Tet (1). Both these homozygous mutant fly lines show only partial lethality, unlike homozygous Tet^{null} flies that are 100% lethal and die as pharate adults in the late pupal stage (**SI Appendix Fig. S2 A, B)**. We analyzed the changes in MB structure in both mutant lines. By staining the adult brains with Fas2 antibody to visualize the α/β lobes, we found that homozygous Tet^{AXXC} showed the β lobe fusion phenotype in 68% (n=37), while, surprisingly, in homozygous Tet^{YRA} the fusion was seen in just 11% (n=35), and wild type had 0% (n=30) β lobe fusion (**Fig.1K-M and N**). Thus, the CXXC zinc finger domain of Tet rather than its 2OGFeDO catalytic domain is primarily required for normal β axon development.

Tet is required for MB axonal guidance in early pupal brain development

The development of the MB starts in early embryogenesis, when it originates from eight neuroblasts (**Fig.2A**). To determine when during development Tet is required, we combined the MB GAL4 driver (201Y) with a temperature sensitive GAL80 ($GAL80^{ts}$), which allows RNAi to be restricted to specific developmental stages. We selectively induced Tet RNAi at white prepupal stage (WPP) to adult, WPP to 48h after puparium formation (APF), or embryo to WPP (**Fig.2B**). Tet RNAi during embryogenesis and larval development does not cause β axon midline crossing (embryo to WPP) but Tet RNAi during pupation (WPP to adult, WPP to 48h APF) resulted in β fusion similar to what is observed when Tet is depleted throughout development (embryo to adult) (**Fig. 2C**). Tet is therefore specifically required in early pupae for normal MB development.

To examine which step in normal brain development requires Tet, Tet^{AXXC} brains were stained with Fas2 antibody to visualize α/β lobes. Based on our observation that β lobe fusion occurred at early pupation (WPP to 48h APF), we looked at the development of these lobes from white prepupae (WPP), at the beginning of the pupal stage, to about halfway through pupal development (48h APF) at 12 hours intervals. We did not observe any β lobe fusion during the first 12h of puparium formation in Tet^{AXXC} brains, but at 24h we observed β axons crossing the midline in the Tet^{AXXC} brains (**Fig. 2D**). The fact that MB structural defects occur during early pupal brain development (12-24h APF) supports the conclusion that Tet is required during the first 24h of pupation to inhibit the MB β axons from crossing the brain midline.

Fas2 staining labels MB axon bundles; however, it cannot reveal how single axons grow. Thus, we employed a stochastic labeling method in which a membrane tethered molecular marker called smGdP (spaghetti monster Green darkened Protein) was put under the control of the GAL4/UAS and heat shock FLP/FRT inducible systems (39). This method has been used to label single neurons, axons, and small dendrites at high resolution (39). To label growing axons, we need a GAL4 driver that is expressed in neurons that have active axon growth. Tet-T2A-GAL4, which is a GAL4 driver expressed under the control of the Tet promoter (40, 41), expresses in such neurons. We expressed smGdP under Tet-T2A-GAL4 control, heat shocked at WPP, and stained brains at 21h APF with anti-HA antibody. The result showed that Tet-T2A-GAL4 labeled a subset of MB neurons, their axons (**SI Appendix Fig. S3A**) and importantly, growing axons (**SI Appendix Fig. S3B-D)** including β axons projecting their growth cone toward the brain midline (**SI Appendix Fig. S3C**). In addition, inducing Tet RNAi by Tet-T2A-GAL4 produced the same β lobe midline crossing phenotype as seen by 201Y-GAL4 driver (**SI Appendix Fig. S4A, B**). Thus, we can use Tet-T2A-GAL4 driver for simultaneously inducing Tet RNAi and labeling growing β axons to see how these axons behave under wild type versus Tet RNAi condition. We found that in Tet RNAi at 21h APF, some axons at the tip of the left β lobe are protruding and extending their projection over the midline toward the right β lobe (**Fig. 2H-J**). This phenomenon does not occur in the control (**Fig. 2E-G**). In this experiment we look at an early time in prospective adult axon outgrowth and therefore the very first axons crossing the midline that will serve as a guide for other axons to cross resulting in the complete fusion we observed in the adult brain (**Fig.1**). In addition to the Tet RNAi axon outgrowth, we also noticed that there are small swellings located along the portion of the axon that crossed the midline (**Fig. K, L,** arrowheads). These swellings are the signs of synaptic boutons indicating that the midline crossing axons, normally restrained to the left-brain hemisphere, likely form synapses with neurons from the right brain hemisphere and potentially affect the MB circuit. Thus, Tet is required to keep β axons confined to one of the two brain hemispheres to prevent any misconnection of β axons between the two sides of the brain.

Tet controls MB axon guidance by regulating glutamine synthetase 2 levels in the brain

To investigate how Tet controls MB axon guidance, 24h pupal brains of *wild-type* and Tet^{AXXC} were dissected and subjected to RNA sequencing to identify genes that are differentially expressed in Tet^{AXXC} mutant versus *wild-type* brains. The result is shown as a volcano plot in which p-value and fold change cut-offs are respectively 0.01 and 2 (**Fig. 3A**). We found that in the Tet^{AXXC} brains, 1503 genes are up-regulated and 29 genes down-regulated compared to wild type (**SI Appendix Table S2 and S1).** The majority of the up-regulated genes are expressed at low levels and GO term analysis showed that these up-regulated genes functioned mostly in sperm development and motility (**SI Appendix Fig. S5A, B**). Among the 29 down-regulated genes in the Tet mutant, the two most significantly reduced genes, the *Glutamine synthetase 2* (*Gs2*) and the *GABA transporter* (*Gat*) are encoding for the key enzymes of glutamatergic signaling and key transporter of GABAergic signaling (**Fig. 3A, B**). Gs2 is the enzyme that converts glutamate to glutamine and Gat is the transporter that can uptake GABA to glial cells (**Fig. 3B**) (42-44). Thus, these two proteins are crucial for regulating and maintaining the levels of glutamate and GABA in the synaptic junction.

To confirm the RNA sequencing results, we performed RT-qPCR of these two genes using RNA from *wild type* and Tet^{AXXC} brains (**Fig. 3C**). The result confirmed that both *Gs2* and *Gat* are down-regulated in Tet^{AXXC} (**Fig. 3C**). In addition,

previous studies have shown that Fmr1 mutants also exhibit the β lobe fusion phenotype (23, 45). Thus, we also dissected 24h pupal brains of *Fmr1*^{3} mutant (29) to test the expression of these same two genes. Interestingly, *Gs2* and *Gat* are also down-regulated in *Fmr1*^{3} (**Fig. 3C**). The observations that *Tet* and *Fmr1* mutants have similar MB phenotypes, and that *Gs2* and *Gat* are reduced in brains of both mutants, suggests that Tet might regulate MB axon guidance via glutamatergic and GABAergic signaling.

Glutamate can control the growth rate of dopaminergic axons (24) and can also reduce the responsiveness of growth cones to repellent cues (25). Further, GABA has been shown to control axonal growth (26, 27). Thus, the down-regulation of *Gs2* and *Gat* may be responsible for the MB axon midline crossing phenotype. To test this hypothesis, we induced *Gs2* and *Gat* RNAis under the control of the MB driver 201Y-GAL4 to see whether this recapitulates the *Tet*^{AXXC} mutant phenotype. *Gs2* RNAi produced the β lobe axon midline crossing phenotype (**Fig. 3H-M and N**), similar to the phenotype observed in *Tet*^{AXXC} brains. However, due to lethality that occurred in *Gat* RNAi animals, we were not able to determine the requirement of *Gat* in regulating MB axon guidance. Thus, we focused on *Gs2* for further experiments.

To confirm the *Gs2* RNAi phenotype, we employed CRISPR/Cas9-mediated mutagenesis to inactivate the *Gs2* gene ubiquitously. The mutagenesis is mediated by the combination of a ubiquitous Cas9 expression driver Act5C-Cas9 and a ubiquitous Gs2 sgRNA expression stock. To validate that the Gs2 protein level was reduced by this approach we performed western blots of extracts from control and mutagenized third instar larval brains. The mutagenized brains showed a significant reduction of Gs2 protein compared to control brains (**Fig. 3D**). Importantly, forty-five percent of the *Gs2* mutagenized brains showed MB with midline axon crossing while no control brains showed this phenotype (**Fig. 3E, F, and G**). These results are consistent with Tet controlling MB axon guidance by regulating the level of Gs2 during brain development.

Tet acts in insulin-producing cells to regulate MB axon guidance

Inducing *Tet* or *Gs2* RNAi in 201Y-GAL4 expressing cells produces a MB midline crossing phenotype. However, exactly which cells in the brain express Gs2 to control MB organization is not known. In early pupal brains (24h APF), 201Y-GAL4 expresses in both MB neurons and a group of cells at the midline of the brain (**Fig. 4A**). To examine if the MB neurons or midline cells express Gs2, brains were stained with anti-Gs2 antibody (46). In brains expressing CD8::GFP driven by 201Y-GAL4, the Gs2 antibody does not stain the MB neurons (**Fig. 4B-D**) but instead stain possibly glial cell that wraps around the calyx region (**Fig. 4B-D**). Gs2 expression is not detected in the midline region between the two growing β lobes (**SI Appendix Fig. S6A-C**). Surprisingly, Gs2 was strongly expressed in the midline cells identified by 201Y-Gal4 (**Fig. 4E-G**). In fact, most of the midline cells express Gs2 (**Fig. 4E-G**, asterisks). A different MB driver, OK107-GAL4, is expressed in both the MB neurons and the insulin-producing cells (IPCs), which are located at the brain midline (47). In addition, Cao et al., have shown that Gs2 is highly enriched in IPCs (48). Thus, we suspected that the midline cells identified by 201Y-GAL4 are IPCs and therefore Tet regulates Gs2 in these cells to control MB axon guidance. To test this hypothesis, we induced Tet or Gs2 RNAis using a Dilp2-GAL4 driver, which is expressed specifically in IPCs. Inducing *Tet* or *Gs2* RNAi in the IPCs produced an MB axon crossing phenotype similar to that observed in *Tet*^{AXXC} (compare **Fig. 4I, J, and K** to control **Fig. 4H and K**). This result confirms that IPCs are the cells in which Tet and Gs2 act to regulate MB axon guidance.

Axon guidance defects in *Tet*^{AXXC} are modulated by glutamatergic signaling

Gs2 is a key enzyme in the glutamatergic pathway in the brain. Reduction of Gs2 levels may lead to the accumulation of glutamate and a deficiency of glutamine in the brain. Excess amounts of glutamatergic signaling have been proposed as the main cause of Fragile X syndrome (49). In fact, the MB midline crossing phenotype in the *Fmr1*^{3} mutant can be rescued by treating the flies with metabotropic glutamate receptor (mGluR) antagonist MPEP (23) or enhanced by treating the flies with glutamate (50). The observation that *Tet*^{AXXC} has the same phenotype as *Fmr1*^{3} led us to examine if the MPEP and glutamate treatments could also rescue the MB crossing defect of the *Tet*^{AXXC} mutant. Third instar larvae were transferred to food supplemented with MPEP or glutamate as treatments, or water as control (**Fig. 5A**). The treatment had no negative effect on viability (**SI Appendix Fig. S7**). Brains from 5 to 10-day-old flies were dissected and stained with Fas2 antibody and the percentage of brains showing MB midline crossing was quantified. The result showed that treating *Tet*^{AXXC} mutants with glutamate enhanced the number of flies with the midline crossing phenotype by 27% compared to the non-treated control (**Fig. 5B**). This indicates that glutamate levels affect the development of MB axons in *Tet*^{AXXC} mutants. Treating *Tet*^{AXXC} mutants with MPEP showed a 17% reduction of the β lobe fusion phenotype (**Fig. 5B**). Neither

of the treatments affected wild-type flies (**Fig.5B**) Thus, modulating the glutamatergic signaling by glutamate or the mGluR antagonist MPEP can worsen or suppress the MB axon midline crossing in *Tet*^{AXXC} mutant brains.

Axon guidance defects in *Tet* and *Fmr1* mutants are suppressed by Gs2 expression

We observed that Gs2 is strongly reduced in *Tet*^{AXXC} and *Fmr1*^{3} brains, and we hypothesized that supplying Gs2 via a transgene could help the brain to overcome this deficit and rescue MB structural defects. This was tested utilizing the same Dilp2-GAL4 driver used in the *Gs2* RNAi experiments described above (**Fig. 4H-K**). For these rescue experiments, *Tet*^{AXXC} mutants that expressed Gs2 in the IPCs (*Dilp2-GAL4/UAS-Gs2; Tet*^{AXXC}*/ Tet*^{AXXC}) (**Fig. 5E**) were compared to the mutant control, *Tet*^{AXXC} mutants that did not express Gs2 (*Dilp2-GAL4/+; Tet*^{AXXC}*/ Tet*^{AXXC}) (**Fig. 5D**) and the wild-type control (*Dilp2-GAL4/+*) (**Fig. 5C**). The same experimental design was applied to rescue *Fmr1*^{3} mutants (**Fig. 5C-E**). Results showed that while Dilp2-GAL4 alone did not affect the MB phenotype, expressing Gs2 in *Tet*^{AXXC} brains can significantly reduce the phenotype (26% MB fusion) compared to *Tet*^{AXXC} flies without Gs2 expression (47% MB fusion, **Fig.5F**). Furthermore, when Gs2 is expressed in *Fmr1*^{3} mutant brains, the structural defect was similarly reduced (21% MB fusion) compared to the homozygous mutant *Fmr1*^{3} brains (54% MB fusion, **Fig. 5G**). Taken together, these results indicate that supplying additional Gs2 to the IPCs under the control of Dilp2-GAL4 driver in the homozygous *Tet*^{AXXC} or *Fmr1*^{3} mutant brain prevents the MB defect caused by these mutants. This result points out that downregulation of Gs2 plays a key role in structural defects in the *Tet* and *Fmr1* mutant brains. It also suggests that Tet and Fmr1 may coordinate with each other to control the expression of Gs2.

Discussion

Tet is highly expressed in nerve cells in embryos and larvae and Tet RNAi knockdown shows diverse neurological phenotypes (7). In this study, we have expanded our understanding of Tet's neural functions by determining that Tet regulates axon guidance in the early developing brain via glutamatergic signaling and that overexpressing Gs2, a key enzyme of the pathway, can rescue axonal defects in Tet and Fmr1 mutant brains.

Tet is required for mushroom body β lobe axon guidance during early brain development

Our results establish that Tet is required for the normal development and guidance of axons in the mushroom body (MB), a prominent structure of the brain that controls a variety of neurological functions such as learning, memory, circadian rhythm, sleep, and courtship (16, 17). Tet is essential for the separation of axons at the midline, which prevents fusion of β lobes. This function appears to be mainly controlled by the CXXC DNA-binding domain as a mutation in this domain, *Tet*^{AXXC}, exhibits the same β lobe fusion phenotype observed in Tet RNAi brains, while the catalytic domain mutant, *Tet*^{YRA}, has a limited contribution to controlling MB axon guidance. TET is essential for neurodevelopment (51); however, the requirement of the Tet DNA-binding domain in axon guidance has not been described before. Our study reveals a new function of Tet in regulating axon guidance in the brain via its CXXC DNA-binding domain.

Tet is required during early pupal brain development (~24h APF) for normal MB axon guidance. This is also the time point when the β axons grow to form the mature MB β lobes. The result underlines that the protein is required at a specific stage during axonal growth to guide these new axons to the right destination during brain development. Our results also show that the requirement for Tet function in the MB β axonal outgrowth and guidance is limited to the first 48 hours of pupal brain development. The finding also has an important application for treating neurodevelopmental disorders in which the treatment needs to be applied at early ages for better interventions.

Careful inspection of the Tet RNAi axons that cross the midline showed that these axons formed small swellings, which is a sign of synaptic boutons, in the “wrong” brain hemisphere. Synaptic boutons are the sites where axons connect, illustrating that in Tet RNAi brains, the circuits of the hemispheres are misconnected. Thus, our data further show that Tet controls axon guidance to prevent abnormal axonal connections from forming in the early-developing brain.

Tet regulates glutamatergic signaling by controlling Gs2 levels

Our RNA-seq and RT-qPCR results demonstrated that Gs2 and Gat are regulated by Tet. Gs2 is a key enzyme in regulating glutamate levels in glutamatergic signaling and Gat is the neurotransporter that controls GABA levels in the GABAergic signaling suggesting that Tet is required in both pathways. The function of Gat in controlling axon development needs to be further elucidated due to the lethal phenotype in Gat knockdown animals. Inducing Gs2 RNAi by MB driver 201Y-GAL4 resulted in axonal defect phenotype indicating that MB axon guidance is regulated by glutamatergic

signaling via Gs2. In addition, treating *Tet*^{AXXC} mutants with MPEP, a metabotropic glutamate receptor (mGluR) antagonist (23), can rescue the axon β lobe fusion phenotype while glutamate treatment enhances the *Tet*^{AXXC} phenotype. These data uncover a new function of Tet in regulating glutamatergic signaling in the brain and support the notion that the pathway is mis-regulated in Tet mutant brains. Glutamatergic signaling is a major excitatory signal in the human brain and the pathway is also known to act in neural developmental events such as proliferation, differentiation, migration, and synaptogenesis (21). Interestingly, elevated levels of glutamatergic signaling have also been proposed as the underlying mechanism of the neurodevelopmental disorder in Fragile X syndrome (49). Based on the conserved functional domains of Tet in humans and flies, the mis-regulation of the glutamatergic signaling during early brain development may also occur in individuals harboring Tet mutations causing neurodevelopmental disorders.

We have previously mapped Tet-DNA binding sites in the genome by ChIP-seq and mapped Tet-mediated 5hmrC RNA modification throughout the transcriptome by hMeRIP-seq (52). There is no Tet binding detected by ChIP-seq on the gene body or promoter region of *Gs2* and *Gat* (**SI Appendix Fig. S9)**. In addition, the Gs2 and Gat mRNAs do not carry the Tet-dependent 5hmC modification (52). These observations suggest that Tet regulates *Gs2* and *Gat* indirectly. Since *Gs2* and *Gat* are also downregulated in the *Fmr1*^{3} mutant, *Tet* and *Fmr1* may function together to control the mRNA levels of these two genes. Fmr1 was previously found in the regulatory protein complex Not1/CCR4 (53), which is known to control all steps of gene expression from transcription in the nucleus to mRNA degradation in the cytoplasm depending on the associated proteins that interact with the complex (54). We have previously also identified Fmr1 in a complex with Zfrp8 (Zinc finger protein RP-8), which functions in the formation of mRNA ribonucleoprotein (mRNP) complexes (55). Interestingly, Zfrp8 was co-immunoprecipitated with Tet (**SI Appendix Fig. S10**). Thus, Tet and Fmr1 may both coordinate with the Not1/CCR4 or other mRNP complexes to regulate mRNA levels of *Gs2* and *Gat* genes.

The importance of Gs2 levels in insulin-producing cells (IPCs) for β lobe axon guidance

IPCs in *Drosophila* are a group of neurons located at the dorsal midline of the central brain that functions in producing and secreting insulin-like peptides to the hemolymph to regulate growth and metabolism (56, 57). Previous studies showed that IPCs can also regulate neuronal functions (58, 59). For instance, overexpressing Fmr1 in IPCs could rescue the circadian defects observed in *Fmr1* mutants (52). But whether the IPCs can regulate MB axonal development has not been elucidated. In our RNA-seq experiments, *Gs2* is the most significantly reduced transcript in the *Tet*^{AXXC} mutant brain. We found that Gs2 is expressed in the IPCs but not in MB neurons. We also observed the midline-crossing phenotype when we specifically knock down either Tet or Gs2 in IPCs. Hence our results point to a previously unknown function of IPCs in regulating MB axon guidance via glutamatergic signaling in the developing brain.

Knockdown of Tet or Gs2 in IPCs resulted in the same phenotype observed in the *Tet*^{AXXC} mutant. This result shows that Tet is required primarily in the IPCs to control the level of Gs2 that is essential to influence the guidance of the β lobe axons. Gs2 is expressed in glial cells where it is responsible for converting glutamate to glutamine to regulate the levels of the neurotransmitter glutamate in the brain (60, 61); however, it is also known to be highly expressed in IPCs (48). Thus, the reduction of Gs2 levels in *Tet*^{AXXC} mutant may lead to the accumulation of glutamate and a deficiency of glutamine in the brain causing axonal defects. However, the mechanism by which Tet and Gs2 regulate axon guidance needs to be further elucidated. One possible mechanism is that, in Tet mutant brains, Gs2 is reduced in the IPCs leading to the accumulation of glutamate in the IPCs that is then secreted at the brain midline (model in **Fig. 6**). The elevated levels of glutamate at the midline could cause MB β axons to cross over the midline. Consistent with this model, glutamate has been reported to reduce the responsiveness of axonal growth cones to repellent cues such as Slit-2 and Sema-3A/C (25) and also can enhance the growth rate and branching of dopaminergic axons (24). In addition, glutamate can be released by pancreatic cells, which are the insulin secreting cells in mammals, via excitatory amino acid transporters (EAAT) by uptake reversal (62). The uptake reversal activity of EAAT has also been reported in astrocyte and it depends on the relative intracellular and extracellular glutamate concentration (63). However, further studies need to be conducted to test the secretion of glutamate by IPCs, and to investigate whether the MB β axon crossing phenotype is due to elevated glutamate levels at the midline of *Tet*^{AXXC} mutant brains.

Tet and Fmr1 overlapping functions and Gs2 rescue phenotype

MPEP was successfully used to suppress the axonal defect in *Fmr1*^{3} mutants (23) while high glutamate concentration can enhance the phenotype (50). Our observation that MPEP and glutamate have similar effects on the *Tet*^{AXXC} animals suggests that Tet and Fmr1 have overlapping functions. This conclusion is further strengthened by our finding that Gs2 is downregulated in the brain of both *Tet*^{AXXC} and *Fmr1*^{3} mutants, and that supplying additional Gs2 by

over-expressing it from a transgene reduced the occurrence of the β lobe fusion phenotype in both *Tet*^{AXXC} and *Fmr1*^{3} mutant brains (**Fig. 5C-G**). The Gs2 rescue phenotype also demonstrates that Gs2 levels are pivotal for regulating axonal guidance at the midline of the brain (**Fig. 6**). The rescue of the axon defect phenotype is only partial. This may be because the level of Gs2 expression is crucial, or because other targets of Tet and Fmr1 contribute to the phenotype. As Tet and Fmr1 can regulate a broad spectrum of genes, it is impressive that overexpression of only one gene, Gs2, encoding a key enzyme in the glutamatergic pathway, can rescue the axonal defect in roundly half of both *Tet* and *Fmr1* mutant animals. Dysfunction of glutamatergic signaling is involved in a variety of human diseases including Fragile X syndrome, autism spectrum disorder, schizophrenia, neurodegenerative diseases, and gliomas (49, 64-66).These results suggest that glutamine synthetase is a potential target for early intervention. Recently, an increasing number of studies have shown that Tet mutations are associated with neurodevelopmental disorders in humans (9-12). The mechanism by which human TET mutations cause these disorders needs to be further elucidated, but the highly conserved functional domain of human and *Drosophila* Tet suggests that Tet function in axon guidance may be conserved in humans. Thus, our study provides initial evidence that glutamatergic signaling is altered in the Tet mutant brains of an animal model and proposes further studies on mammalian systems for drug screening and treatment of neurodevelopmental disorders caused by TET mutations.

Materials and Methods

Drosophila stocks

Fly stocks were cultured on the standard food medium at 25 °C. The following stocks were obtained from Bloomington Drosophila Stock Center (BDSC): UAS-mCD8::GFP, 201Y-GAL4 driver (#64296)(32), enhancer trap Tet-T2A-GAL4-pA (#76666) (41), multicolor flip-out stock MCFO-2 (#64086) (39), Act5C-Cas9 (#54590), Gs2 sgRNA for Gs2 CRISPR/Cas9 mutagenesis (#76492), Gs2 RNAi (#92838) (67), Gat RNAi (#29422), mCherry RNAi (#35785), tubP-GAL80^{ts} (#7017), and UAS-Dcr2 (#24651). Tet RNAi lines were obtained from Vienna Drosophila Resource Center (VDRC, GD#14330 and KK#108964). Dilp2-GAL4 was originally obtained from Dr. Eric Rulifson (University of California, San Francisco) (56). Fmr1^{3} mutant was kindly provided by Dr. Thomas A. Jongens (University of Pennsylvania) (29).

Temperature shift GAL80^{ts}

The driver 201Y-GAL4 was crossed with *Tet RNAi (*GD#14330*); GAL80ts* or *mCherry RNAi; GAL80ts* to generate Tet knockdown GAL80ts or mCherry RNAi control GAL80ts. The crosses and progenies were kept at 18ºC or 29ºC following the temperature shift scheme detailed in (**Fig. 2B**). Five to ten days old adult brains were dissected and stained to calculate the percentage of β fusion phenotype on each condition.

Generating Tet^{AXXC} and Tet^{YRA} mutants

The *Tet*^{AXXC} mutant was generated using the scarless gene editing approach which is mediated by CRISPR/Cas9 cut and homologous directed repair (HDR) of the designed DNA template harboring targeted mutations (35-37). Two gRNAs (gRNA1 and gRNA2) were designed to bind to both sides of the CXXC zinc finger domain flanking regions to guide the Cas9 cut. These gRNAs were synthesized (IDT, USA) and cloned to the pU6-BbsI-chiRNA expression vector (Addgene #45946)(37). The two homology arms were generated by PCR from the nos-Cas9 stock (BDSC # 54591) genomic DNA. The PCR was done using gene-specific and mutated primers to generate one wild-type homology arm and one mutated homology arm with at least 1000 bp overlap with the flanking genomic DNA from the cut site (Fig. S7). The homology arms were cloned to the pScarlessHD-DsRed donor vector (Addgene # 64703, gift from Kate O'Connor-Giles). The mixture of these vectors was injected into the nos-Cas9 stock and screened for the DsRed marker. DsRed positive lines were genetically crossed to remove the non-Cas9 chromosome. Then, these lines were crossed to a piggyBac recombinase stock 3xP3-ECFP, alpha-tub-piggyBacK10/TM6C, Sb^{1} (BDSC # 32072) to excise the DsRed marker. The mutant stocks were validated by PCR and Sanger sequencing. The *Tet*^{YRA} mutant was generated using the same method. The sequences for sgRNAs and primers to generate homology arms are listed in **SI Appendix Table S3**.

Simultaneously knockdown and visualizing axons of Tet expressing cells

The Tet enhancer trap line Tet-T2A-GAL4-pA (41) was used as Tet-T2A-GAL4 driver to drive Tet knockdown at Tet-expressing cells in the pupal brain and labeling cell body as well as axons of these cells. The knockdown can be accomplished because Tet-T2A-GAL4-pA was inserted between exons 5 and 6 but the RNAi stock construct

(KK#108964) was bound to exon 8 (**SI Appendix Fig. S8**). The poly(A) (pA) signal will trigger the transcriptional termination to ensure the RNAi will not bind and degrade the transcript containing the GAL4 coding sequence. To inducible label axons with high resolution, we employed the MCFO2 stock which can expresses membrane tethered smGdPs (spaghetti monster Green darkened Proteins) under the control of both GAL4/UAS and heat shock FLP/FRT inducible systems (39). smGdP is a darkened chromophore Green Protein fused with multiple copies of epitope tag (e.g., HA, V5, OLLAS, FLAG, and Myc) and a myristoylation for better visualization of small axons and dendrites (68). The Tet RNAi stock (KK#108964) or mCherry RNAi were crossed to the flip-out stock MCFO-2 to generate *UAS-Tet RNAi; MCFO-2* or *UAS-mCherry RNAi; MCFO-2* stocks. Then, Tet-GAL4 was crossed to the *UAS-Tet RNAi; MCFO-2* for Tet knockdown and labeling axons of Tet expressing neurons, or *UAS-mCherry RNAi; MCFO-2* for the control. The crosses were kept at 25ºC to produce white pupae. Then, white pupae were collected and placed on the wall of the *Drosophila* glass vials. The vials were heat shocked for 3 minutes at 37ºC in a water bath, then transferred to a 25ºC incubator and grown for 21 hours. Then, pupal brains were dissected and immunostained for visualizing the growing MB axons.

Brain dissection and immunostaining

Brain dissection and immunostaining were performed as previously described (69) with the following modifications. Adult brains were dissected in cold 1X phosphate-buffered saline (PBS) and fixed in 4% formaldehyde at 25ºC for 20 min on a slow rotator (7 rpm). Pupa brains were dissected in cold 1X PBS, then immediately transferred to a cold fixation solution containing 4% formaldehyde diluted in Schneider's *Drosophila* Medium (Gibco # 21720024) kept on ice. The pupa brains can be kept in the cold fixation solution for a maximum of one hour. Then these pupa brains were fixed at 25ºC for 45 min on a slow rotator (7 rpm). After fixing, brains were quickly washed with 0.3% PBS-T (0.3% Triton-X100 in 1X PBS) one time, then three washes with 0.3% PBS-T, 20 min each. The brains were blocked in blocking solution (0.15% PBS-T containing 10% normal goat serum) at 25 °C for 20 min. These brains were then incubated with the following primary antibodies diluted in blocking solution: mouse anti-Fasciclin II (Fas2, DSHB #1D4, deposited by Corey Goodman, 1:50), rabbit anti-GFP (Invitrogen #A-11122, 1:1000), mouse anti-glutamine synthetase (GS) antibody, clone GS-6 (Millipore-Sigma #MAB302, 1:1000) at 4 °C overnight or rabbit anti-HA (Invitrogen #MA5-27915, 1:1000) at 4°C over two nights. After primary antibody incubation, the brains were washed with 0.3% PBS-T, 3 times for 20 minutes each. Then, brains were incubated with secondary antibodies conjugated with Cy3 (Jackson ImmunoResearch #115-165-003, 1:400), Cy5 (Jackson ImmunoResearch #711-175-152, 1:400), or Alexa 488 (Invitrogen # A-11001, 1:400) at 4 °C overnight or over two nights (Fig. 2E-L). Brains were washed 3 times, 20 min each with 0.3% PBS-T followed by 2 quick washes with 1X PBS. The brains were mounted in Vectashield mounting medium (Vector Laboratories # H-1000-10) in SecureSeal imaging spacers (Electron Microscopy Sciences #70327-9S). Brains were imaged using Leica SP8 confocal microscope (Leica Microsystem) and deconvoluted using either Lightning Deconvolution (Leica Microsystem) or Huygens Confocal Deconvolution (Scientific Volume Imaging). The images were processed using Fiji (70).

Total RNA isolation

Pupal brains were dissected in PBS and immediately frozen on dry ice. Totally, 30 brains per genotype were collected at 24h APF (After Puparium Formation). Three independent biological replicates per genotype were used for RNA isolation. Total RNA was isolated using RNeasy Plus Universal Kit (QIAGEN, USA) following the manufacturer's instructions including DNase I treatment using RNase-Free DNase Set and on-column protocol (QIAGEN, USA). The isolated total RNAs were aliquoted for both RNA-seq and qRT-PCR.

Quantitative reverse transcription PCR (RT-qPCR)

One microgram of total RNA from wild-type, Tet, and Fmr1 mutants was reserve transcribed to cDNA using MMLV High-Performance Reverse Transcriptase Kit (Biosearch Technologies #RT80125K) and oligo(dT) primers (IDT). The cDNAs were used for real-time quantitative PCR using gene-specific primers with Rpl32 as the internal reference control (**SI Appendix Table S4**) and PowerUp SYBR Green Master Mix (Applied Biosystems #A25741) with StepOnePlus Real-Time PCR System (Applied Biosystems). The relative quantification (RQ) for the expression of each gene was calculated using the comparative Ct method (71).

RNA-seq library generation

Library preparation and sequencing were performed at Novogene. One microgram of total RNA was used as input for library preparation. Prior to library preparation, total RNA quality was validated for the following parameters: degradation

and contamination using 1% agarose gel electrophoresis, purity by NanoPhotometer® spectrophotometer (IMPLEN, USA), and integrity using Bioanalyzer 2100 and RNA Nano 6000 Kit (Agilent Technologies, USA). Sequencing libraries were generated using NEBNext® Ultra™ Directional RNA Library Prep Kit for Illumina® (NEB, USA) following the manufacturer's instruction. mRNA was purified from total RNA using oligo dT magnetic beads. Purified mRNAs were fragmented by divalent cations. First-strand cDNA synthesis using random hexamer and M-MuLV RT (RNase H-). The dUTP method was used to synthesize the second strand and generate a strand-specific library. After 3' A overhangs were cleaved by exonuclease, DNA fragments were ligated with NEBNext® hairpin loop adaptor to prepare for hybridization. AMPure XP system (Beckman Coulter, USA) was used for 150-200 bp size selection. The size selected and purified products were treated with USER® Enzyme to open up the NEBNext adapter. Then, PCR was performed with Phusion High-Fidelity DNA polymerase using Universal PCR primers and Index (X) prime. PCR products were purified using the AMPure XP system and quality was assessed by Agilent Bioanalyzer 2100. Clustering was done using cBot Cluster System using PE Cluster Kit cBot-HS (Illumina, USA) according to the manufacturer's recommendation. Sequencing was performed on Illumina Novaseq 6000 (Illumina, USA) to generate paired-end reads.

RNA-seq data analysis

Raw reads were filtered and trimmed by Trimmomatic 0.39 (72). Then, the filtered reads will be mapped to Ensembl *Drosophila melanogaster* genome assembly BDGP6.22 using HISAT2 (73). The mapping SAM files were converted to BAM using Samtools (74). The number of reads mapped to the individual gene is counted by featureCounts (75). Differential gene expression analysis was done by DESeq2 (76). Then, the result was visualized by the Bioconductor package EnhancedVolcano (77).

Western blot

Thirty L3 instar larval brains from Act5C-GAL4 driving Gs2 CRISPR/Cas9 mutagenesis or Act5C-GAL4 wild-type control were dissected and immediately frozen on dry ice. Total protein was isolated from these brains using RIPA buffer (25 mM Tris HCl pH 7.6, 150 mM NaCl, 1% NP-40, 1% sodium deoxycholate, 0.1% SDS; Thermo Scientific #89900) supplemented with 1X Protease Inhibitor Cocktail (Roche # 5892791001) and 25ug of the total protein was loaded to each well. Glutamine synthetase antibody, clone GS-6 (Millipore-Sigma #MAB302) was used at 1: 2000 dilution and beta-tubulin antibody, clone TU27 (BioLegend # 903401) was used at 1: 1000 dilution. The western blot signals were detected using anti-mouse IRDye 800CW Infrared Dyes conjugated secondary antibody in the LICOR Odyssey CLx imaging system. Signals were quantified using LICOR Image Studio Lite software.

MPEP and glutamate treatment

Wild type and Tet^{AXXC} mutant were grown in the standard medium at 25°C to early third instar larva. Then, sixty larvae were collected and transferred to a vial containing MPEP- or glutamate-supplemented medium at 100 µM or water-supplemented medium as diluent control. Twelve hours after transferring, larvae that came out from the medium will be eliminated to ensure all larvae will consume the supplemented medium for at least 12 hours. This allows the larvae to uptake MPEP or glutamate before they begin to pupate and stop eating. The larvae that stayed inside the medium were continuing to grow into adults. Then, the adult flies after eclosion were transferred back to the standard medium. Five to ten days old adult brains were dissected and immunostained to quantify the percentage of MB β lobe fusion per each condition.

Gs2 rescue stocks

Gs2 cDNA was obtained from DGRC clone LP04559 (DGRC #1337593). The coding region was amplified by Phusion Hot Start II HF (Thermo Scientific # F565S) using gene-specific primers with homology arms designed for DNA Assembly: Gs2.RB.armR.Eco (gccgcagatctgttaacgctattcgtccaggcagatggt) and Gs2.RB.armL.Eco (gaactctgaatagggaattgggcaacatgcattccgcgatcctggag). The amplicon was cloned to the pUASTattB expression vector (DGRC #1419, deposited by Bischof and Basler) at the EcoRI restriction site by NEBuilder HiFi DNA Assembly Cloning Kit (NEB #E5520S). The pUASTattB-Gs2 vector was injected to *y^1 w^{67c23}; PCaryPattP40* stock (78) by the BestGene company to insert the UAS-Gs2 construct to attP40 landing site on the second chromosome. The *UAS-Gs2* stock was screened by the mini-white marker and validated by genomic PCR and Sanger sequencing.

UAS-GS2 stock was crossed with Tet^{AXXC} and $Fmr1^3$ mutants to generate *UAS-Gs2; Tet^{AXXC}/TM6B Tb^1* and *UAS-Gs2; $Fmr1^3$/TM6B Tb^1*. The Tet^{AXXC} and $Fmr1^3$ mutants were also crossed with the Dilp2-GAL4 driver to generate *Dilp2-*

GAL4; Tet^{AXXC}/TM6 Sb^{1} and *Dilp2-GAL4; Fmr1^{3}/TM6 Sb^{1}*. Then, the stocks will be crossed to generate rescued stocks and respective controls. The progenies were collected after eclosion, separated to eliminate balancers, transferred to fresh medium, and dissected at five to ten days old for MB β lobe immunostaining and quantification.

Statistical Analysis

Chi-square test for two or more categories were done using GraphPad Prism version 9.5.1 (GraphPad Software, San Diego, California USA). Statistical analysis of RNA-seq data was done using R.

Acknowledgments

We thank Kenneth Irvine, Cordelia Rauskolb, and Nicholas Stavropoulos for helpful comments on the manuscript. We want to thank Fei Wang, Kishan Bulsara, Anna Zhang, Ethan Chiang for preliminary data. Irvine, Barber, and Stavropoulos labs for helpful discussion and technical supports, and Thomas A. Jongens and Eric Rulifson for fly stocks. We thank Svetlana Minakhina for co-IP result in Figure S10. We also thank Drosophila Genomics Resource Center, Bloomington Drosophila Stock Center, Vienna Drosophila Resource Center, and Developmental Studies Hybridoma Bank for cDNA, fly stocks, and antibodies. This work was supported by grants from the National Institute of Health (R01 GM118404 to R.S.), the Vietnam Education Foundation (VEF) and Charles and Johanna Busch Pre-doctoral Fellowships (to H.T.).

References

1. M. Tahiliani *et al.*, Conversion of 5-methylcytosine to 5-hydroxymethylcytosine in mammalian DNA by MLL partner TET1. *Science* **324**, 930-935 (2009).
2. K. D. Rasmussen, K. Helin, Role of TET enzymes in DNA methylation, development, and cancer. *Genes Dev* **30**, 733-750 (2016).
3. L. Fu *et al.*, Tet-mediated formation of 5-hydroxymethylcytosine in RNA. *J Am Chem Soc* **136**, 11582-11585 (2014).
4. B. Delatte *et al.*, RNA biochemistry. Transcriptome-wide distribution and function of RNA hydroxymethylcytosine. *Science* **351**, 282-285 (2016).
5. B. N. Singh *et al.*, Tet-dependent 5-hydroxymethyl-Cytosine modification of mRNA regulates the axon guidance genes robo2 and slit in Drosophila. *bioRxiv* 10.1101/2023.01.03.522592, 2023.2001.2003.522592 (2023).
6. T. L. Dunwell, L. J. McGuffin, J. M. Dunwell, G. P. Pfeifer, The mysterious presence of a 5-methylcytosine oxidase in the Drosophila genome: possible explanations. *Cell Cycle* **12**, 3357-3365 (2013).
7. F. Wang *et al.*, Tet protein function during Drosophila development. *PLoS One* **13**, e0190367 (2018).
8. H. Q. Dai *et al.*, TET-mediated DNA demethylation controls gastrulation by regulating Lefty-Nodal signalling. *Nature* **538**, 528-532 (2016).
9. D. B. Beck *et al.*, Delineation of a Human Mendelian Disorder of the DNA Demethylation Machinery: TET3 Deficiency. *Am J Hum Genet* **106**, 234-245 (2020).
10. R. Seyama *et al.*, Two families with TET3-related disorder showing neurodevelopmental delay with craniofacial dysmorphisms. *J Hum Genet* **67**, 157-164 (2022).
11. R. L. P. Santos-Cortez *et al.*, Novel candidate genes and variants underlying autosomal recessive neurodevelopmental disorders with intellectual disability. *Hum Genet* **137**, 735-752 (2018).
12. R. Harripaul *et al.*, Mapping autosomal recessive intellectual disability: combined microarray and exome sequencing identifies 26 novel candidate genes in 192 consanguineous families. *Mol Psychiatry* **23**, 973-984 (2018).
13. I. Farhy-Tselnicker, N. J. Allen, Astrocytes, neurons, synapses: a tripartite view on cortical circuit development. *Neural Dev* **13**, 7 (2018).
14. E. C. Engle, Human genetic disorders of axon guidance. *Cold Spring Harb Perspect Biol* **2**, a001784 (2010).
15. N. J. Strausfeld, L. Hansen, Y. Li, R. S. Gomez, K. Ito, Evolution, discovery, and interpretations of arthropod mushroom bodies. *Learn Mem* **5**, 11-37 (1998).
16. Y. Aso *et al.*, Mushroom body output neurons encode valence and guide memory-based action selection in Drosophila. *Elife* **3**, e04580 (2014).

17. Q. Li, H. Jang, K. Y. Lim, A. Lessing, N. Stavropoulos, insomniac links the development and function of a sleep-regulatory circuit. *Elife* **10** (2021).
18. T. Kunz, K. F. Kraft, G. M. Technau, R. Urbach, Origin of Drosophila mushroom body neuroblasts and generation of divergent embryonic lineages. *Development* **139**, 2510-2522 (2012).
19. G. Riedel, B. Platt, J. Micheau, Glutamate receptor function in learning and memory. *Behav Brain Res* **140**, 1-47 (2003).
20. M. P. Mattson, Glutamate and neurotrophic factors in neuronal plasticity and disease. *Ann N Y Acad Sci* **1144**, 97-112 (2008).
21. R. Lujan, R. Shigemoto, G. Lopez-Bendito, Glutamate and GABA receptor signalling in the developing brain. *Neuroscience* **130**, 567-580 (2005).
22. P. Y. Wang, R. S. Petralia, Y. X. Wang, R. J. Wenthold, S. D. Brenowitz, Functional NMDA receptors at axonal growth cones of young hippocampal neurons. *J Neurosci* **31**, 9289-9297 (2011).
23. S. M. McBride *et al.*, Pharmacological rescue of synaptic plasticity, courtship behavior, and mushroom body defects in a Drosophila model of fragile X syndrome. *Neuron* **45**, 753-764 (2005).
24. Y. Schmitz, J. Luccarelli, M. Kim, M. Wang, D. Sulzer, Glutamate controls growth rate and branching of dopaminergic axons. *J Neurosci* **29**, 11973-11981 (2009).
25. T. A. Kreibich, S. H. Chalasani, J. A. Raper, The neurotransmitter glutamate reduces axonal responsiveness to multiple repellents through the activation of metabotropic glutamate receptor 1. *J Neurosci* **24**, 7085-7095 (2004).
26. S. Eins, P. E. Spoerri, E. Heyder, GABA or sodium-bromide-induced plasticity of neurites of mouse neuroblastoma cells in culture. A quantitative study. *Cell Tissue Res* **229**, 457-460 (1983).
27. G. Barbin, H. Pollard, J. L. Gaïarsa, Y. Ben-Ari, Involvement of GABAA receptors in the outgrowth of cultured hippocampal neurons. *Neurosci Lett* **152**, 150-154 (1993).
28. M. R. Santoro, S. M. Bray, S. T. Warren, Molecular mechanisms of fragile X syndrome: a twenty-year perspective. *Annu Rev Pathol* **7**, 219-245 (2012).
29. T. C. Dockendorff *et al.*, Drosophila lacking dfmr1 activity show defects in circadian output and fail to maintain courtship interest. *Neuron* **34**, 973-984 (2002).
30. Y. Q. Zhang *et al.*, Drosophila fragile X-related gene regulates the MAP1B homolog Futsch to control synaptic structure and function. *Cell* **107**, 591-603 (2001).
31. F. V. Bolduc, K. Bell, H. Cox, K. S. Broadie, T. Tully, Excess protein synthesis in Drosophila fragile X mutants impairs long-term memory. *Nat Neurosci* **11**, 1143-1145 (2008).
32. C. Redt-Clouet *et al.*, Mushroom body neuronal remodelling is necessary for short-term but not for long-term courtship memory in Drosophila. *Eur J Neurosci* **35**, 1684-1691 (2012).
33. K. Williams *et al.*, TET1 and hydroxymethylcytosine in transcription and DNA methylation fidelity. *Nature* **473**, 343-348 (2011).
34. R. Deplus *et al.*, TET2 and TET3 regulate GlcNAcylation and H3K4 methylation through OGT and SET1/COMPASS. *Embo j* **32**, 645-655 (2013).
35. S. J. Gratz, J. Wildonger, M. M. Harrison, K. M. O'Connor-Giles, CRISPR/Cas9-mediated genome engineering and the promise of designer flies on demand. *Fly (Austin)* **7**, 249-255 (2013).
36. S. J. Gratz *et al.*, Highly specific and efficient CRISPR/Cas9-catalyzed homology-directed repair in Drosophila. *Genetics* **196**, 961-971 (2014).
37. S. J. Gratz *et al.*, Genome engineering of Drosophila with the CRISPR RNA-guided Cas9 nuclease. *Genetics* **194**, 1029-1035 (2013).
38. J. H. Lee, K. S. Voo, D. G. Skalnik, Identification and characterization of the DNA binding domain of CpG-binding protein. *J Biol Chem* **276**, 44669-44676 (2001).
39. A. Nern, B. D. Pfeiffer, G. M. Rubin, Optimized tools for multicolor stochastic labeling reveal diverse stereotyped cell arrangements in the fly visual system. *Proc Natl Acad Sci U S A* **112**, E2967-2976 (2015).
40. F. Diao *et al.*, Plug-and-play genetic access to drosophila cell types using exchangeable exon cassettes. *Cell Rep* **10**, 1410-1421 (2015).
41. P. T. Lee *et al.*, A gene-specific T2A-GAL4 library for Drosophila. *Elife* **7** (2018).

42. C. Caggese, P. Barsanti, L. Viggiano, M. P. Bozzetti, R. Caizzi, Genetic, molecular and developmental analysis of the glutamine synthetase isozymes of Drosophila melanogaster. *Genetica* **94**, 275-281 (1994).
43. M. S. Thimgan, J. S. Berg, A. E. Stuart, Comparative sequence analysis and tissue localization of members of the SLC6 family of transporters in adult Drosophila melanogaster. *J Exp Biol* **209**, 3383-3404 (2006).
44. R. Chaturvedi, T. Stork, C. Yuan, M. R. Freeman, P. Emery, Astrocytic GABA transporter controls sleep by modulating GABAergic signaling in Drosophila circadian neurons. *Curr Biol* **32**, 1895-1908.e1895 (2022).
45. C. I. Michel, R. Kraft, L. L. Restifo, Defective neuronal development in the mushroom bodies of Drosophila fragile X mental retardation 1 mutants. *J Neurosci* **24**, 5798-5809 (2004).
46. I. Sinakevitch, Y. Grau, N. J. Strausfeld, S. Birman, Dynamics of glutamatergic signaling in the mushroom body of young adult Drosophila. *Neural Dev* **5**, 10 (2010).
47. L. E. Enell, N. Kapan, J. A. Söderberg, L. Kahsai, D. R. Nässel, Insulin signaling, lifespan and stress resistance are modulated by metabotropic GABA receptors on insulin producing cells in the brain of Drosophila. *PLoS One* **5**, e15780 (2010).
48. J. Cao *et al.*, Insight into insulin secretion from transcriptome and genetic analysis of insulin-producing cells of Drosophila. *Genetics* **197**, 175-192 (2014).
49. M. F. Bear, K. M. Huber, S. T. Warren, The mGluR theory of fragile X mental retardation. *Trends Neurosci* **27**, 370-377 (2004).
50. S. Chang *et al.*, Identification of small molecules rescuing fragile X syndrome phenotypes in Drosophila. *Nat Chem Biol* **4**, 256-263 (2008).
51. I. C. MacArthur, M. M. Dawlaty, TET Enzymes and 5-Hydroxymethylcytosine in Neural Progenitor Cell Biology and Neurodevelopment. *Front Cell Dev Biol* **9**, 645335 (2021).
52. B. N. Singh *et al.*, Tet-dependent 5-hydroxymethyl-Cytosine modification of mRNA regulates the axon guidance genes robo2 and slit in Drosophila. *bioRxiv* 10.1101/2023.01.03.522592 (2023).
53. C. Temme *et al.*, Subunits of the Drosophila CCR4-NOT complex and their roles in mRNA deadenylation. *RNA* **16**, 1356-1370 (2010).
54. M. A. Collart, The Ccr4-Not complex is a key regulator of eukaryotic gene expression. *Wiley Interdiscip Rev RNA* **7**, 438-454 (2016).
55. W. Tan, C. Schauder, T. Naryshkina, S. Minakhina, R. Steward, Zfrp8 forms a complex with fragile-X mental retardation protein and regulates its localization and function. *Dev Biol* **410**, 202-212 (2016).
56. E. J. Rulifson, S. K. Kim, R. Nusse, Ablation of insulin-producing neurons in flies: growth and diabetic phenotypes. *Science* **296**, 1118-1120 (2002).
57. D. R. Nässel, Insulin-producing cells and their regulation in physiology and behavior of Drosophila. *Canadian Journal of Zoology* **90**, 476-488 (2012).
58. A. F. Barber, R. Erion, T. C. Holmes, A. Sehgal, Circadian and feeding cues integrate to drive rhythms of physiology in Drosophila insulin-producing cells. *Genes Dev* **30**, 2596-2606 (2016).
59. D. R. Nässel, O. I. Kubrak, Y. Liu, J. Luo, O. V. Lushchak, Factors that regulate insulin producing cells and their output in Drosophila. *Front Physiol* **4**, 252 (2013).
60. D. E. Featherstone, E. Rushton, K. Broadie, Developmental regulation of glutamate receptor field size by nonvesicular glutamate release. *Nat Neurosci* **5**, 141-146 (2002).
61. A. Martinez-Hernandez, K. P. Bell, M. D. Norenberg, Glutamine synthetase: glial localization in brain. *Science* **195**, 1356-1358 (1977).
62. N. Feldmann *et al.*, Reduction of plasma membrane glutamate transport potentiates insulin but not glucagon secretion in pancreatic islet cells. *Mol Cell Endocrinol* **338**, 46-57 (2011).
63. C. M. Anderson *et al.*, Differing effects of substrate and non-substrate transport inhibitors on glutamate uptake reversal. *J Neurochem* **79**, 1207-1216 (2001).
64. T. D. Prickett, Y. Samuels, Molecular pathways: dysregulated glutamatergic signaling pathways in cancer. *Clin Cancer Res* **18**, 4240-4246 (2012).
65. T. Miladinovic, M. G. Nashed, G. Singh, Overview of Glutamatergic Dysregulation in Central Pathologies. *Biomolecules* **5**, 3112-3141 (2015).
66. M. Montanari, G. Martella, P. Bonsi, M. Meringolo, Autism Spectrum Disorder: Focus on Glutamatergic Neurotransmission. *Int J Mol Sci* **23** (2022).

67. A. L. Strauss, F. Kawasaki, R. W. Ordway, A Distinct Perisynaptic Glial Cell Type Forms Tripartite Neuromuscular Synapses in the Drosophila Adult. *PLoS One* **10**, e0129957 (2015).
68. S. Viswanathan *et al.*, High-performance probes for light and electron microscopy. *Nat Methods* **12**, 568-576 (2015).
69. H. H. Tran *et al.*, Drosophila Ubiquitin C-Terminal Hydrolase Knockdown Model of Parkinson's Disease. *Sci Rep* **8**, 4468 (2018).
70. J. Schindelin *et al.*, Fiji: an open-source platform for biological-image analysis. *Nat Methods* **9**, 676-682 (2012).
71. K. J. Livak, T. D. Schmittgen, Analysis of relative gene expression data using real-time quantitative PCR and the 2(-Delta Delta C(T)) Method. *Methods* **25**, 402-408 (2001).
72. A. M. Bolger, M. Lohse, B. Usadel, Trimmomatic: a flexible trimmer for Illumina sequence data. *Bioinformatics* **30**, 2114-2120 (2014).
73. D. Kim, J. M. Paggi, C. Park, C. Bennett, S. L. Salzberg, Graph-based genome alignment and genotyping with HISAT2 and HISAT-genotype. *Nat Biotechnol* **37**, 907-915 (2019).
74. H. Li *et al.*, The Sequence Alignment/Map format and SAMtools. *Bioinformatics* **25**, 2078-2079 (2009).
75. Y. Liao, G. K. Smyth, W. Shi, The R package Rsubread is easier, faster, cheaper and better for alignment and quantification of RNA sequencing reads. *Nucleic Acids Res* **47**, e47 (2019).
76. M. I. Love, W. Huber, S. Anders, Moderated estimation of fold change and dispersion for RNA-seq data with DESeq2. *Genome Biol* **15**, 550 (2014).
77. K. Blighe *et al.*, EnhancedVolcano: Publication-ready volcano plots with enhanced colouring and labeling. R package version 1.16.0. *R package version 1.16.0* 10.18129/B9.bioc.EnhancedVolcano (2022).
78. M. Markstein, C. Pitsouli, C. Villalta, S. E. Celniker, N. Perrimon, Exploiting position effects and the gypsy retrovirus insulator to engineer precisely expressed transgenes. *Nat Genet* **40**, 476-483 (2008).

Figures and legends

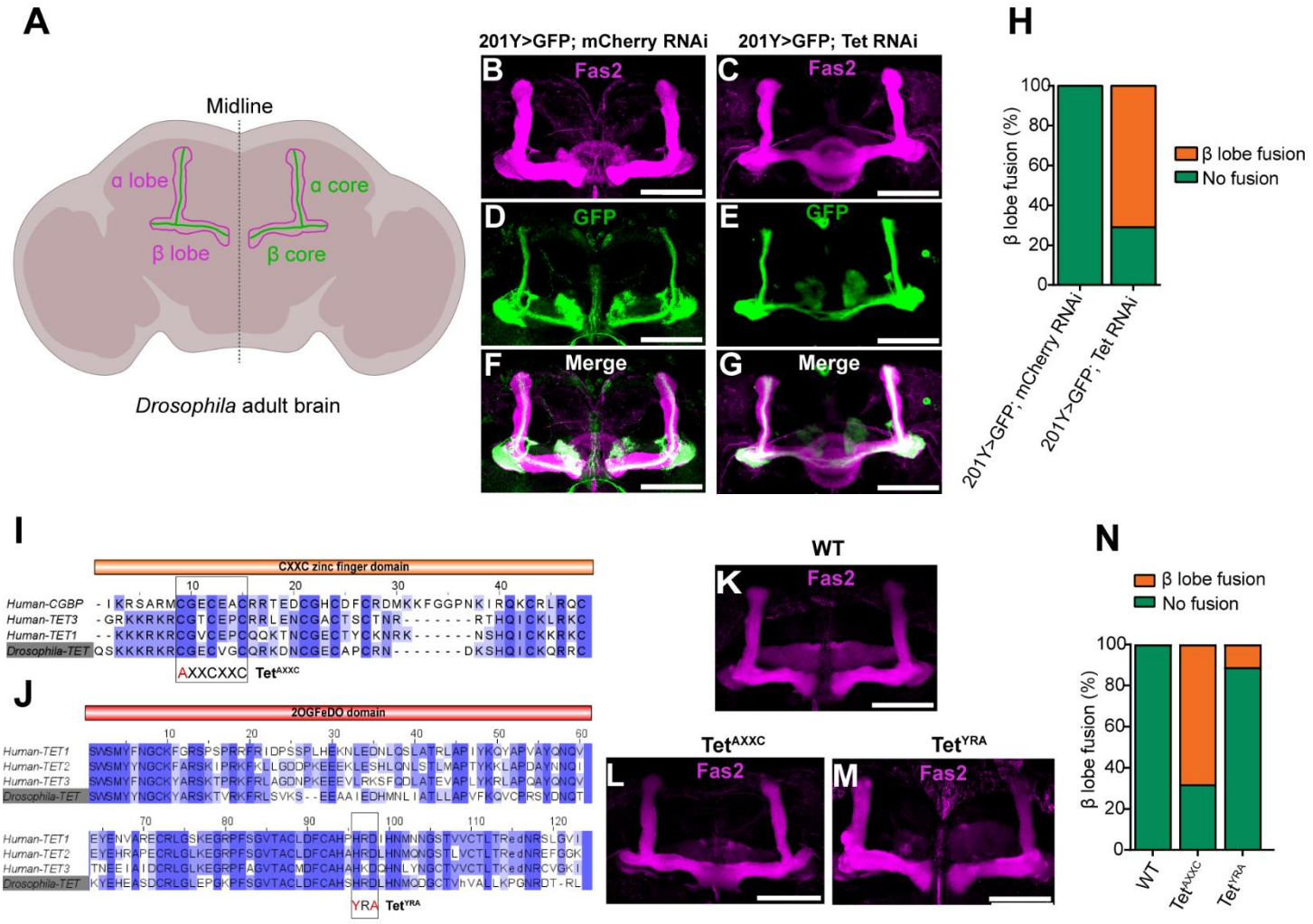

Figure 1. Tet and its CXXC zinc finger domain are required for proper MB β axon development. (**A**) Schematic representation of the adult MB α/β lobe structure and the brain midline, the whole α/β lobes are stained with Fas2 antibody (magenta), α/β core axons are labeled by membrane tagged CD8::GFP driven by MB 201Y-GAL4 driver (green). (**B-G**) Tet knockdown (KD) using the 201Y-GAL4 MB driver, which also controls the expression of membrane-tethered CD8::GFP. α/β lobes were stained with anti-Fas2 antibody (B, C, magenta), α/β cores were stained with anti-GFP antibody (D, E, green), F and G are merged images of B and D or C and E. (**H**) Percentage of β fusion phenotype obtained from RNAi control or Tet KD in (B-G). (**I**) Sequence homology and amino acid conservation of Tet and CGBP CXXC zinc finger DNA-binding domains. (**J**) Sequence homology and amino acid conservation of human and *Drosophila* Tet 2OGFeDO domains. (**K-M**) MB α/β lobes stained with the anti-Fas2 antibody of Tet domain mutants: CXXC zinc finger domain C to A mutation (Tet^{AXXC}), or 2OGFeDO domain HRD to YRA mutation (Tet^{YRA}). (**N**) Quantification of (K-M), percentage of normal or β fusion phenotypes. Scale bar: 50 µm.

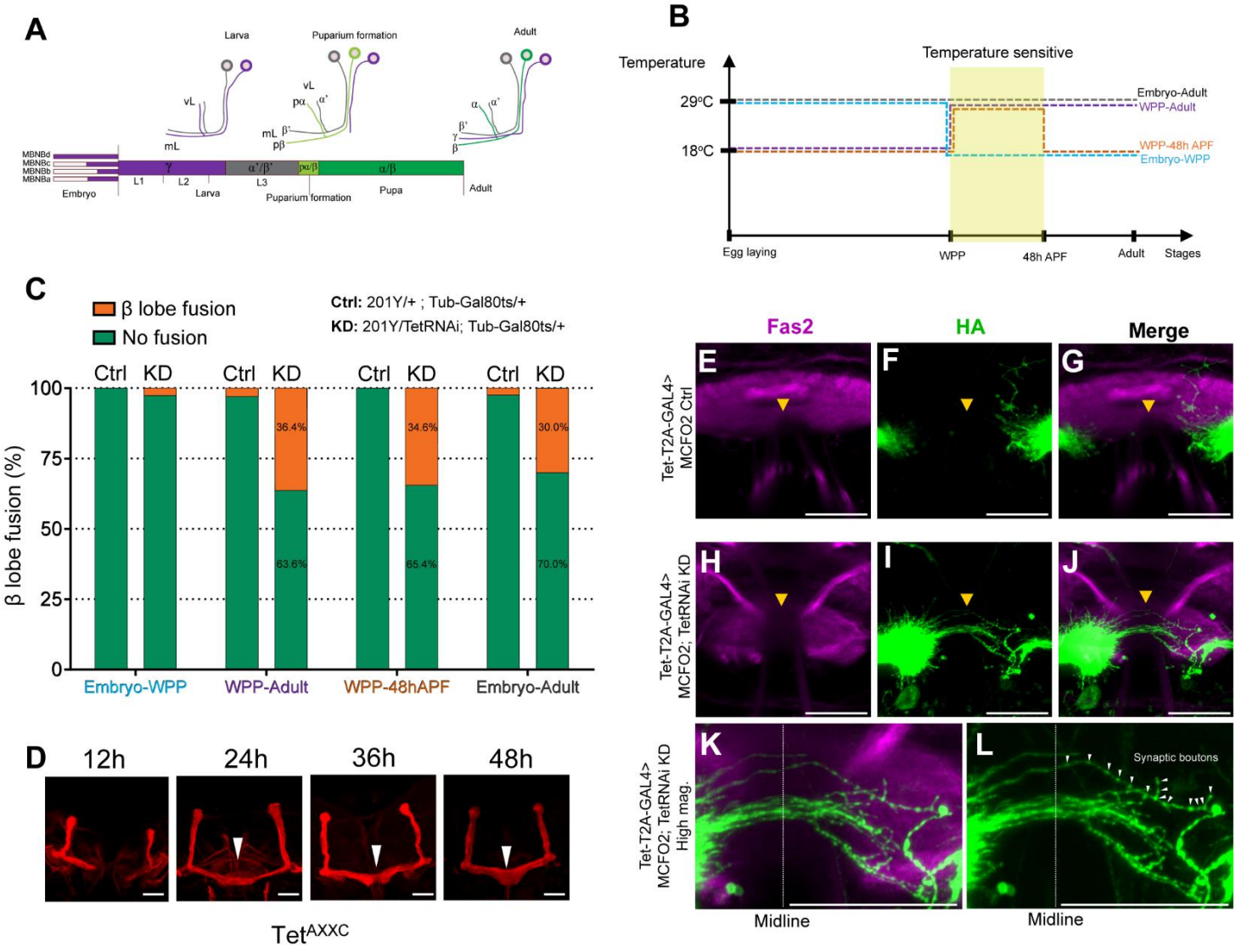

Figure 2. Loss of Tet causes MB axons to cross the midline during early pupal brain development. (**A**) The progression of MB structural development from four embryonic MB neuroblasts (MBNBs) is simplified and depicted following the Kunz et.al. 2012 study (19). (**B**) Temperature shift (TS) scheme to knockdown Tet using the GAL4/GAL80^{ts} system at four developmental stages: embryo to adult, WPP to adult, WPP to 48h APF, embryo to WPP. WPP: white prepupa, APF: after puparium formation. (**C**) Percentage of brains with β lobe midline crossing phenotype (orange) in TS Tet KD (201Y> TetRNAi; tub-GAL80^{ts}, KD) and control (201Y> tub-GAL80ts, Ctrl). Tet KD from embryo to WPP does not affect the growth of β axons, but Tet KD from embryo to adult, WPP to adult, or WPP to 48h APF resulted in β axon midline crossing. The temperature-sensitive period is indicated in yellow in (**B**). (**D**) Tet^{AXXC} pupal brains from different developmental stages (WPP, 12h, 24h, 36h, 48h APF) were stained with anti-Fas2 antibody. β axon midline crossing occurs from 24h APF onward. (**E-M**) Stochastic labeling of MB β axons in the developing pupal brain (21h APF), Tet KD driven by Tet-T2A-GAL4 (**H-J**, Tet-GAL4> MCFO2, TetRNAi) or control (**E-G**, Tet-GAL4> MCFO2) brains. Brains were stained with HA antibody to label axons (green) and Fas2 antibody (magenta) to label MB and ellipsoid body to identify the brain midline. Tet KD in the developing brain leads to growing axons crossing the midline (**I and J**) not observed in the control (**F and G**). (**K**) and (**L**) are high magnifications of (**J**) and (**I**). Tracing of one axon in (**K**) showing the portion of the axon that has crossed the midline. Note the synaptic boutons distributed along it (**L**, arrowhead). Scale bars: 25 µm.

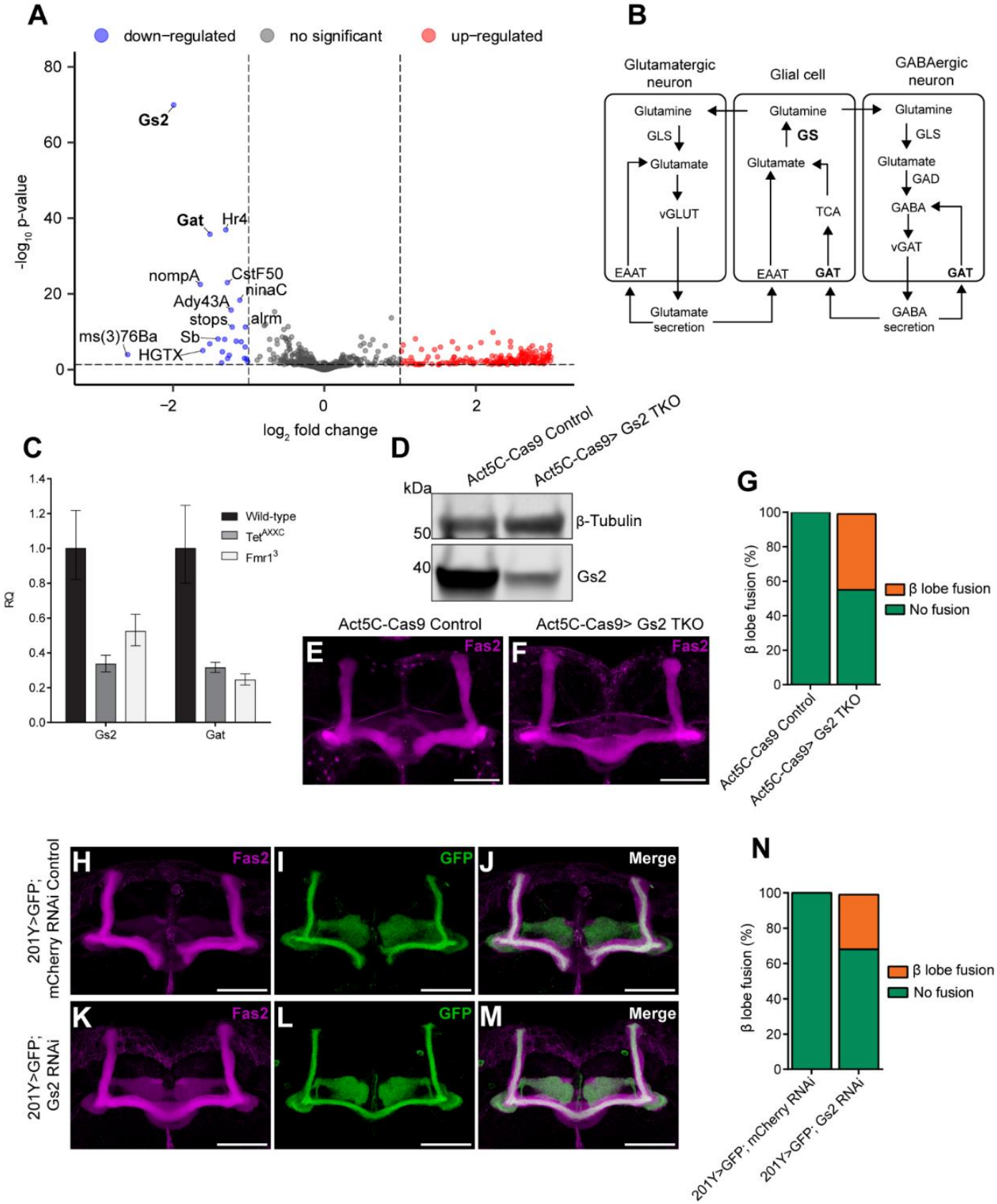

Figure 3. Tet regulates glutamate synthetase 2 levels in the brain and controls MB axon growth. (**A**) Volcano plot of RNA sequencing results, showing differentially expressed RNAs in Tet^{AXXC} and wild-type brain. Significant differences are defined

by p-value < 0.01 and fold change > 2. (**B**) Representation of the glutamatergic and GABAergic pathways showing that Gs2 and Gat are the main enzyme and transporter, respectively, of the pathway. (**C**) Comparison of Gs2 and Gat transcript levels (qRT-PCR) of wild-type or Tet^{AXXC}, and $Fmr1^{3}$ mutant brains. RQ: relative quantification, error bars represent standard deviation (SD). (**D**) Western blot showing Gs2 protein levels in the brains of control (Act5C-Cas9) or CRISPR/Cas9 mutated Gs2 (Act5C-Cas9> Gs2 TKO) blotted with anti- Gs2 antibody. (**E-F**) MB α/β lobes stained with Fas2 antibody showing Gs2 mutated brain exhibiting MB midline crossing (**F**, Act5C-Cas9> Gs2 TKO) not observed in control brains (**E**, Act5C-Cas9 Control). (**G**) Quantification of phenotype seen in (E-F). (**H-M**) Gs2 RNAi KD driven by 201Y-GAL4 (K-M) or control (H-J). All brains express 201-GAL4 driven CD8::GFP. Brains were stained with Fas2 and GFP antibodies to visualize whole α/β lobes (Fas2, magenta) or core α/β (GFP, green). Gs2 KD using MB driver 201Y-GAL4 recapitulates the Tet^{AXXC} midline crossing phenotype not observed in control (K-M). (**N**) Quantification of midline crossing phenotype in (H-M). Scale bars: 50 µm.

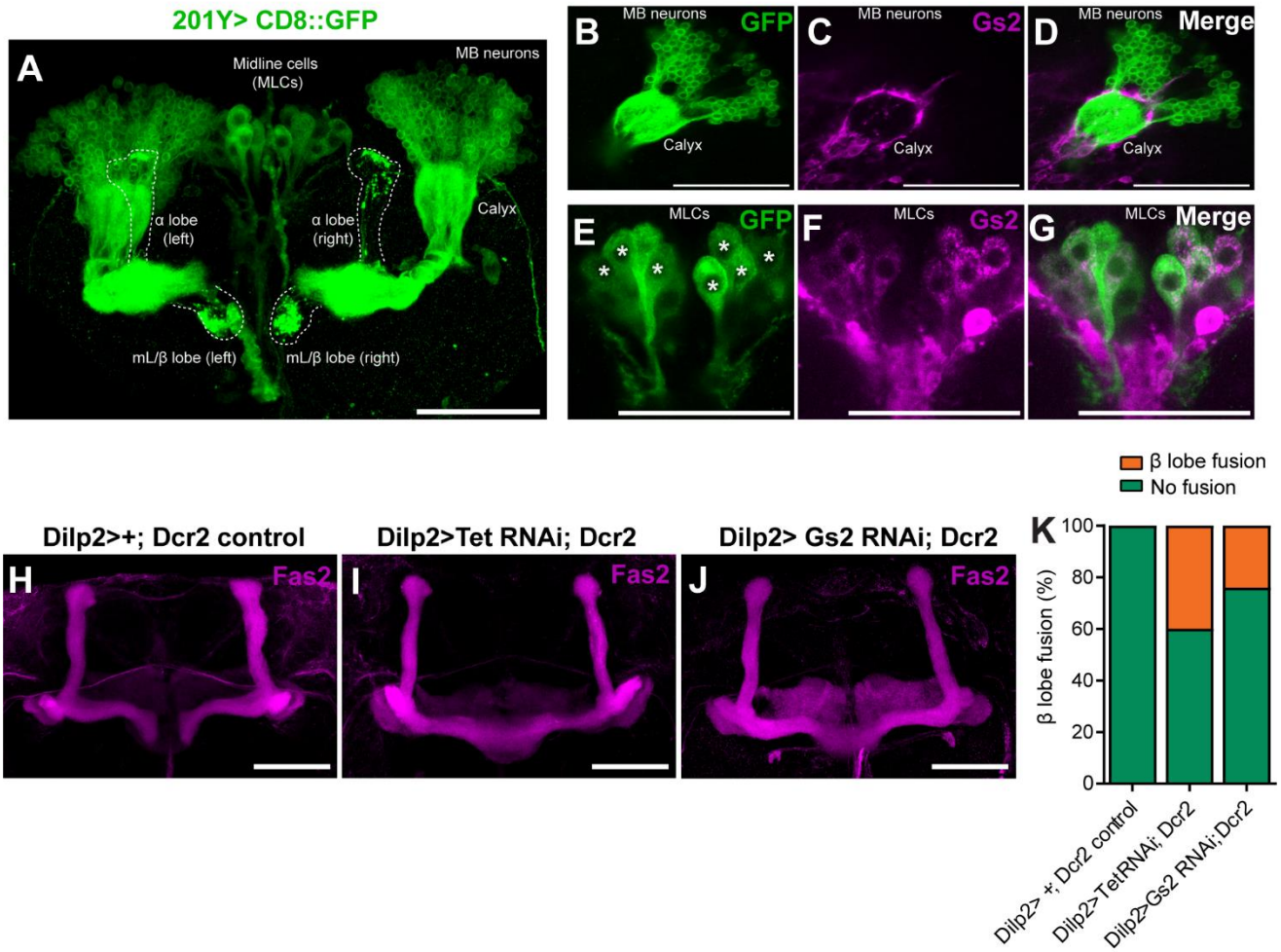

Figure 4. Tet regulates MB axon guidance via insulin-producing cells (IPCs). (**A**) 201Y-GAL4 driven membrane-tagged CD8::GFP expression pattern in 24h APF brain, the driver expresses in MB neurons and midline cells (MLCs). (**B-G**) 201Y-GAL4 driven CD8::GFP cells (green) and Gs2 expressing cells (magenta - anti-Gs2 antibody). Gs2 is not expressed in MB neurons (B-D) but instead is expressed in MLCs (E-G, asterisks marks midline cells expressing Gs2). (**H-J**) MB α/β lobes stained with anti-Fas2 antibody of the Dilp2-GAL4 driver control (H), Dilp2-GAL4 driven Tet KD (I), or Dilp2-GAL4 driven Gs2 KD (J) in IPCs. (**N**) Quantification of β fusion brain in (H-J). Scale bar: 50 µm.

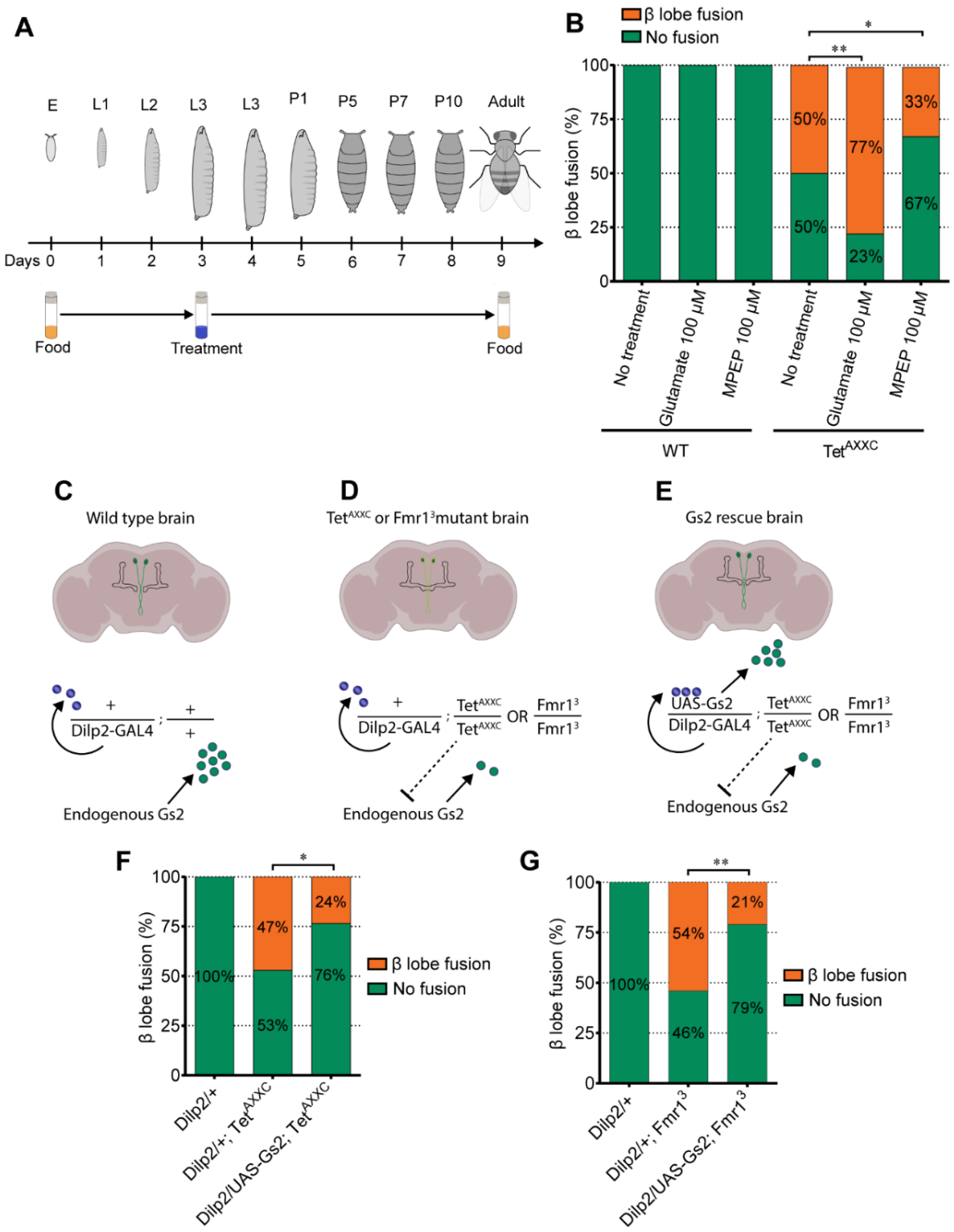

Figure. 5. The *Tet* and *Fmr1* mutant phenotype can be partially rescued by feeding larvae with MPEP or over-expressing Gs2. (**A**) MPEP and glutamate treatment scheme for *Tet*^{AXXC} mutant flies. Third instar larvae are reared on food containing MPEP or glutamate and changed to normal food after eclosion. (**B**) *Wild type* or *Tet*^{AXXC} mutant flies, percentage of MB axon midline crossing brains after MPEP or glutamate treatment. (**C-E**) Schematic representation of the experimental design for rescuing *Tet* or *Fmr1* mutant phenotypes by expressing Gs2 under the control of Dilp2-GAL4. (**F**) Percentage of MB axon midline crossing brains in wild type, *Tet*^{AXXC} mutant, and Gs2 rescued *Tet*^{AXXC} mutant flies. (**G**) Percentage of MB axon midline crossing brains in wild type, *Fmr1*^{3} mutant, and Gs2 rescued *Fmr1*^{3} mutant flies. Chi-square test with * $p < 0.05$, ** $p < 0.01$.

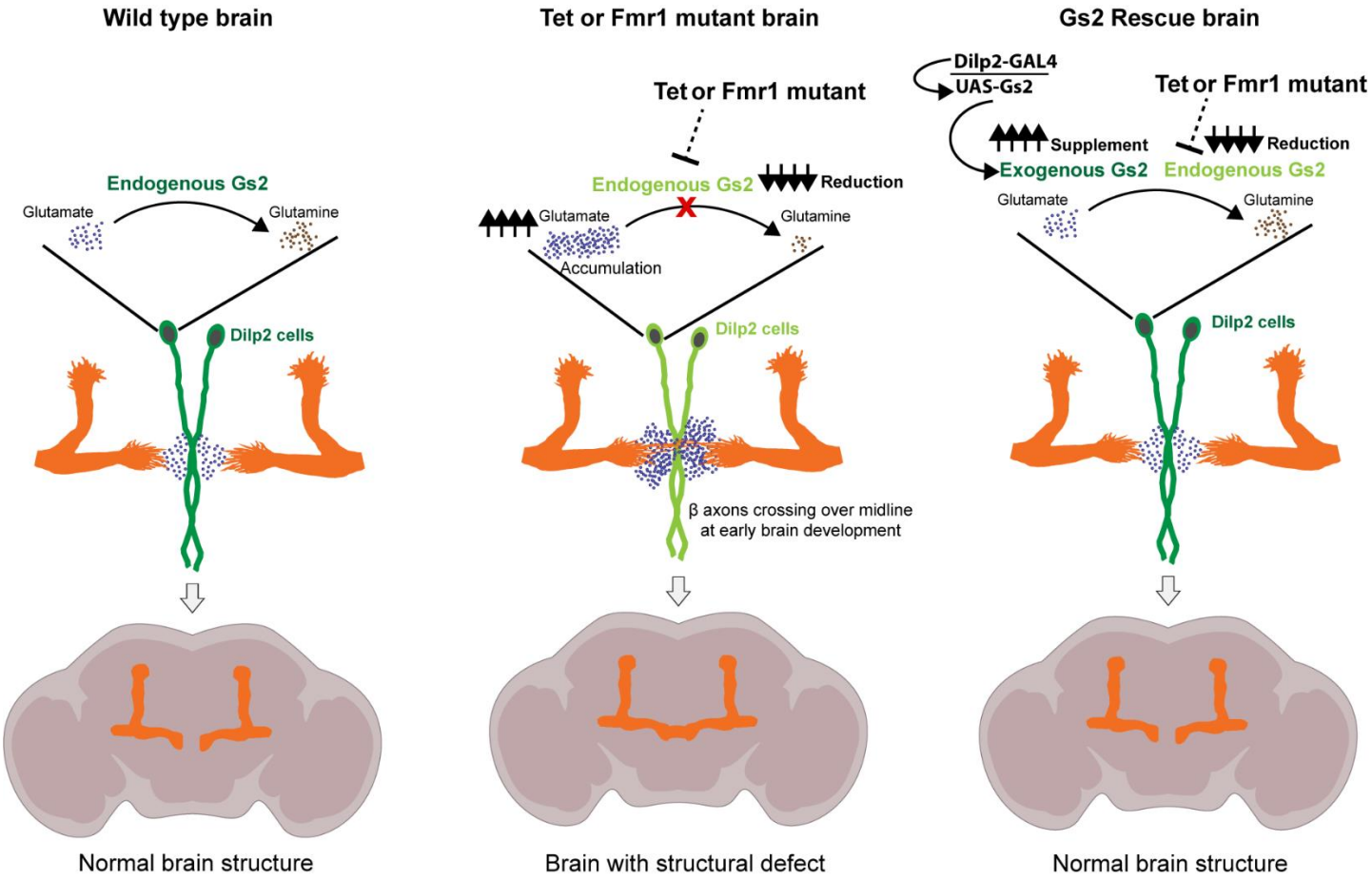

Figure. 6. The model explains how Tet and Fmr1 control MB axon guidance in the brain by regulating the levels of glutamine synthetase 2 (Gs2) and Gs2 overexpression rescues structural defect in Tet and Fmr1 mutant brains.